RSC Advances

ROYAL SOCIETY OF CHEMISTRY

www.rsc.org/advances

Cite this: DOI: 10.1039/c0xx00000x

www.rsc.org/xxxxxx

ARTICLE TYPE

Mesoporous alumina nanosheets and nanorolls derived from topologically identical Al-based MOFs

Yi Liu*,Shucheng Liu, and Zifeng Yue

Received (in XXX, XXX) Xth XXXXXXXXX 20XX, Accepted Xth XXXXXXXXX 20XX

DOI: 10.1039/b000000x

Mesoporous alumina with two kinds of morphologies has been synthesized via the metal-organic frameworks (MOFs) derived route. In this approach, alumina nanosheets and nanorolls were synthesized from two topologically identical Al-based MOFs, MIL-53 and DUT-5, using a two-step calcinations procedure, respectively. The obtained mesoporous alumina exhibits high specific surface area.

Mesoporous metal oxides, as a kind of new functional materials, has very important application in catalysis, separation, adsorption, optoelectronics and environmental fields.[1-7] Among these inorganic materials, alumina is extremely attractive due to their unique properties, such as thermal stability, adsorption behavior and catalytic activity. [8-13] Diverse methods have been applied to the synthesis of mesoporous alumina, e.g. soft templating, hard templating, nanoparticle self-assembly, etc. However among these methods, the high temperatures needed to crystallize the amorphous oxide and remove the template result in collapse of the micropores. It is still a significant challenge to make crystalline alumina that contains large pores.

Porous metal-organic frameworks (MOFs) are coordination polymers consisting of metal ions (or clusters) and organic linkers. These MOFs have attracted much attention due to their wide variety of porous structures.[14-17] The porosity and long-range ordering of MOFs offer an opportunity to synthesize ordering porous oxide.[18-25] A simple pyrolysis method is used for preparing mesoporous metal oxides due to the metal ion coordination can inherit the original spatial structure of MOFs.[26,27] This is a novel route for controllable synthesis and directed assembly of mesoporous metal oxide. Here we report a simple and tunable MOFs-templated strategy by pre-synthetic ligand design for the synthesis of mesoporous alumina. We choose 1,4-benzenedicarboxylic acid (BDC) and biphenyl4,4′-dicarboxylic acid (BPDC) as ligand to construct two kinds of Al-MOF crystal (MIL-53 and DUT-5) under mild solvothermal conditions. Meanwhile, porous alumina was prepared via two-step calcination procedures. Briefly, Al-MOFs was first heated in N_2 gas to obtain black carbon/alumina composite (denoted as C-Al/MIL and C-Al/DUT), then calcinated in O_2 to get the final product of whiter alumina (denoted as Al/MIL and Al/DUT). The carbon matrix formed during carbonization in N_2, in which the metal and metal oxides were embedded. Finally, upon oxidation in O_2 at higher temperature, the carbon matrix evaporated, generating highly porous nanostructures metal oxides.

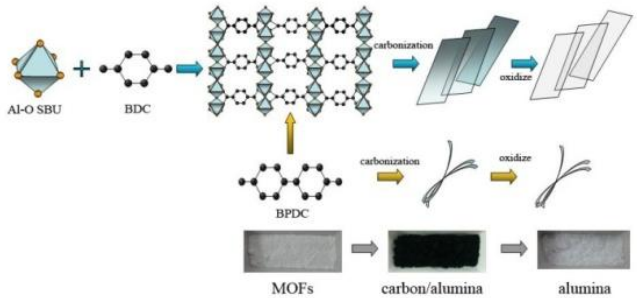

Scheme.1 Illustration of the synthesis procedure for obtaining porous alumina derived from Al-based MOFs

In this approach, the morphologies, textures and porosities of alumina can be controlled by the topological space structure of MIL-53 and DUT-5, which posses same secondary building unit (SBU) and different organic ligand. The change of the organic linker can strongly affect the morphologies of MOFs derived compounds. Two-dimensional alumina nanosheets and one-dimensional nanorolls were formed via the conversion of MIL-53 and DUT-5, respectively. The detailed synthesis strategy for which is visibly depicted in Scheme 1.

The crystal structure of MOFs templates were examined by wide-angle X-ray diffraction (XRD) measurement (Fig.1). The relative intensity and peak positions in the XRD pattern is consistent with previous reports,[28-30] confirming the formation of the crystalline frameworks Al(OH)(bdc) H_2O and Al(OH)(bpdc). MIL-53 is composed of $AlO_4(OH)_2$ octahedra chains by corner sharing, linked to terephthalate ligands to form three-dimensional structures.[29] DUT-5 which is based on biphenyl-4,4′-dicarboxylic acid, is isoreticular to MIL-53, however the rigid framework does not allow breathing of the structure as observed for flexible MIL-53.[30] The XRD pattern of the calcined product C-Al/MIL and Al/MIL is given in Fig.1(a) and Fig.1(b). In contrast to the sharp peaks of the original MOFs crystals, C-Al/MIL particles after carbonization showed broadened and less-resolved peak. This means the frameworks of MIL-53 is collapsed during the carbonization at 550 ℃ in N_2 and the carbon/alumina composite is formed. After thermal treatments of C-Al/MIL at 650 ℃ in O_2, the pure porous alumina was obtained due to the evaporation of carbon. The peaks of Al/MIL

correspond to the γ-alumina phase with a cubic unit cell (JCPDS file No.10-0425). In the case of compounds derived from DUT-5, as shown in Fig.1(c) and (d), the XRD patterns of C-Al/DUT and Al/DUT exhibit more broad diffraction peaks, indicating that the degree of crystallization is lower than that of compounds derived from MIL-53,which should be amorphous alumina phase. No peaks from MOFs or other phase are observed, indicating the high purity of the calcined product.

Thermo gravimetric analysis (TGA) (Fig.S1) shows both MOFs templates decompose at the same temperature range of 500 to 650℃. MIL-53 and DUT-5 were heated evenly and transformed into Al_2O_3 by the departure of BDC and BPDC ligand. During the transformation process, the inorganic building units start to dehydrate gradually and assemble automatically. In this approach, two-step calcinations procedure was using for obtaining the mesoporous alumina. Firstly, the carbon matrix formed during carbonization in N_2, in which the metal and metal oxides were embedded. Secondly, upon oxidation in O_2 at higher temperature, the generated carbon dioxide can release through the channels and pores in precursor. The carbon formed during the thermal decomposition of the MOFs is possibly responsible for stability of frameworks and this carbon can act as the barrier which prevents the particles from agglomerating, induce the uniform pore distribution and relatively high surface area of products.

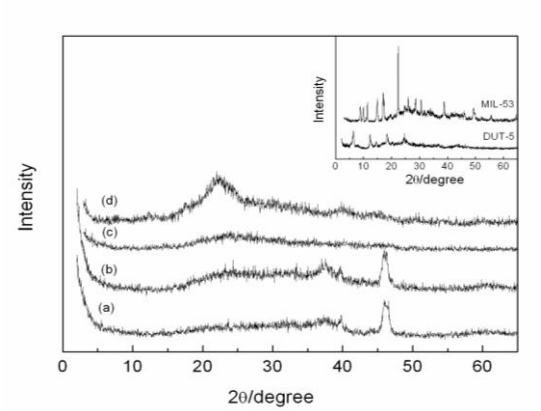

Fig.1 XRD patterns of samples derived from MIL-53 and DUT-5: (a) C-Al/MIL (b) Al/MIL; (c) C-Al/DUT, (d) Al/DUT. The inset shows XRD patterns of MIL-53 and DUT-5

The morphologies and microstructures of the products were also investigated by TEM. The alumina derived from MIL-53 shows typical sheet-like morphology, and channels arranged in parallel can be observed among the sheets (Fig.2), which reflect the regular arrangement of 1D aluminum chains in the precursor. We believe that the formation of nanosheets is actually the outward embodiment of the nature of MIL-53 crystal structure. The structure of MIL-53(Al) consists of a three dimensional framework built up from the interconnection of infinite chains of corner-sharing octahedral $AlO_4(OH)_2$ with 1,4-benzenedicarboxylate ligands.[28] The Al^{3+} is coordinated to four oxygen atoms from four carboxylic groups and two hydroxyl groups located in trans position. The $AlO_4(OH)_2$ units are linked to each other through the two opposite hydroxyl groups and this generates an infinite chain running along the c axis.[28] The two carboxylate functions of each benzenedicarboxylate anion are linked to two distinct adjacent aluminum cations. This connection in the framework generates one dimension channels with large pore sizes. After heating in inert atmosphere, the benzenedicarboxylate (BDC) linker can be gradually broken and the final remainder is transformed into carbon/alumina composites. During the process of elimination of BDC linker, it is proposed that the inorganic building units start to dehydrate gradually and assemble automatically and maintain the layer alignment of their parent MIL-53(Al) with highly arrangements. Hence, when MIL-53 undergoes the hydrothermal process, the final product is always inclined to form nanosheets. However, TEM of products derived from DUT-5 exhibits a one dimensional fiber-like morphology as shown in Fig.3. By careful observation, we found most fibers are the scroll sheets structures. The framework-topology of DUT-5 is isoreticular to MIL-53, however its organic linker is longer than that of MIL-53.[30] It is proposed that the final product derived from DUT-5 under thermal treatment is also always inclined to form nanosheets. However, because the organic ligand length increases, DUT-5 has a larger pore and interlayer spacing between adjacent Al-O octahedral chains than that of MIL-53. Due to increasing the distance between Al-O chains, the sheet morphologies is not stable, tend to curl up. We think that the thermal stress can provide the power for the sheets wrap into rolls. In addition, it is note that the final product (alumina) and intermediate product (carbon/alumina) maintain the similar structures, which indicates that carbon removal have no obvious effect on the frameworks.

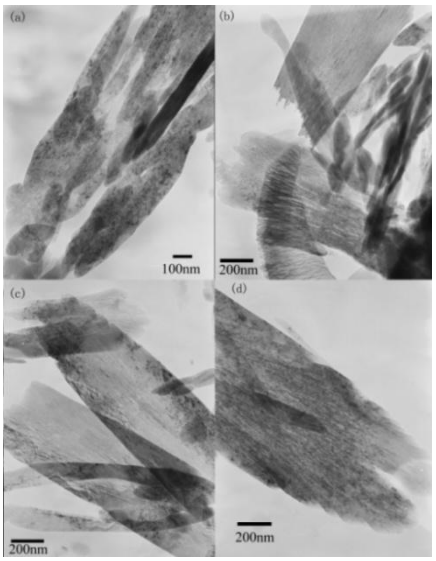

Fig.2 TEM images of samples derived from MIL-53: (a)(b) C-Al/MIL; (c)(d) Al/MIL

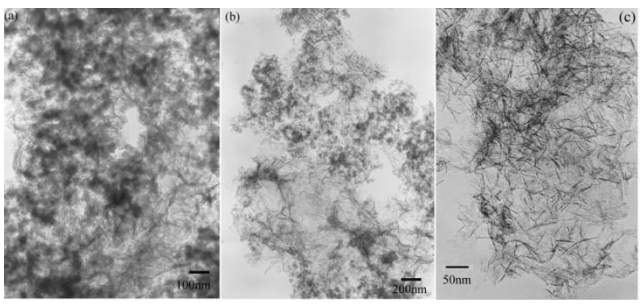

Fig.3 TEM images of samples derived from DUT-5: (a) C-Al/DUT; (b,c) Al/DUT

N_2 adsorption-desorption analysis was carried out to characterize the specific surface area and porosity of the as-prepared samples. As shown in Fig.4, the adsorption-desorption

isotherms of samples exhibit type IV mode, which is related to mesoporous materials. The porosity properties of the samples made by MIL-53 and DUT-5 are summarized in Table S1. Clearly, all the compounds show high BET surface area and total pore volume. Such a high surface area results from high porosity that inherits from the original spatial structure of parent MOFs. The mesopore size distribution curve shows a size distribution about 10-20nm (average pore diameter). Particularly, alumina derived from DUT-5(Al/DUT) has a BET surface area of 269.9 m^2g^{-1} and a total pore volume of 1.397 cm^3g^{-1}, which are significantly higher than those prepared from MIL-53 (88.6 cm^3g^{-1} and 0.259 cm^3g^{-1}). For the alumina derived from MIL-53 it was observed that the porosity is basically made up of channel-like mesopores, as suggested by the hysteresis loop in nitrogen adsorption isotherms and evidenced by the TEM images. On the other hand, the textural properties of DUT-5 derived samples have a curl-shape and the individual fiber exhibits a middle-hollow structure. This makes the adsorption capability of material greatly enhanced. We also note that the BET surface area of alumina slightly higher than that of carbon/alumina composite. This is due to the generated carbon dioxide can release through the channels and pores in precursor upon thermolysis in O_2, generating highly porous nanostructures.

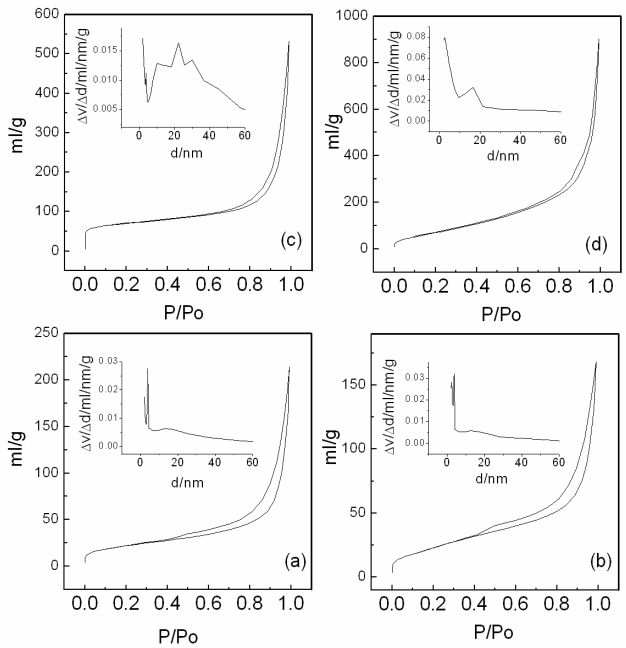

Fig.4 N_2 adsorption-desorption isotherms and BJH pore size distribution of samples: (a) C-Al/MIL; (b) Al/MIL; (c) C-Al/DUT; (d) Al/DUT

We conducted a low pressure static CO_2 adsorption-desorption experiment at 273 K. Fig.5 shows the adsorption-desorption isotherms of samples derived from MIL-53 and DUT-5, respectively. The alumina Al/DUT achieved CO_2 capture capacity up to 18.6 cm^3/g at pressure of 1 bar. The adsorption capacity of sample derived from DUT-5 is noticeably higher than that of sample derived from MIL-53 (14.6 cm^3/g). This can be attributed to the high surface area of sample made by DUT-5, which leads to more adsorption sites exposed to CO_2. However both products show not very high adsorption capacity for CO_2 due to the low pressure (~ 1 bar) condition. It is expected that at high pressure (~ dozens of bar) the obtained alumina will exhibit higher CO_2 adsorption capacity. We will continue to carry out the next step of research. Compared to pure alumina products, the carbon/alumina composites provided a much larger adsorption capacity. This remarkable enhancement of CO_2 adsorption was caused by several factors. The high porosity of the carbon matrix can facilitate fast CO_2 diffusion and promote accessibility to the pore surface. In addition, dispersed Al_2O_3 confined in carbon matrix can provide discrete active sites for CO_2 adsorption. Therefore, increased adsorption sites for CO_2 are expected in carbon/oxides composites made by MOFs, which can lead to an improved CO_2 adsorption performance.

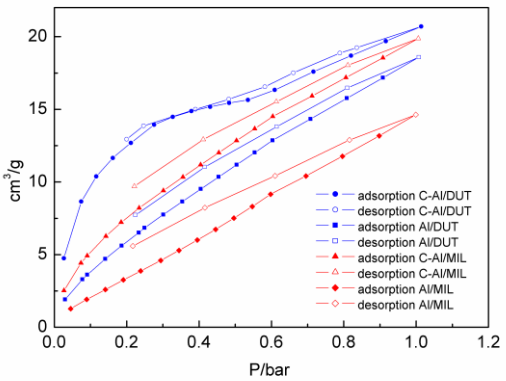

Fig.5 CO_2 adsorption-desorption isotherms of samples at 273K

In summary, we have presented a novel and general synthesis strategy for producing porous alumina with tunable morphologies, size and porosities. Topologically identical MOFs templates MIL-53 and DUT-5 was synthesized by pre-synthetic ligand design. Two-dimensional porous alumina sheet and one-dimensional porous alumina rolled sheet were formed via the calcinations of the MIL-53 and DUT-5. Because of the porous structure inherited from the original MOFs crystals, the as-synthesized mesoporous alumina exhibits high specific surface area. The present synthetic strategy is easily controlled and can be used to prepare other mesoporous metallic oxides.

Acknowledgements

This work was supported by the National Natural Science Foundation of China (21261006), Natural Science Foundation of Guizhou province (2012/2115).

Notes and references

College of Science, Guizhou University, Guiyang 550025, China
E-mail: sci.yiliu@gzu.edu.cn

† Electronic Supplementary Information (ESI) available: [details of any supplementary information available should be included here]. See DOI: 10.1039/b000000x/

1 D.Gu and F. Schüth, *Chem. Soc. Rev.*, 2013,**43**,313.
2 S.M.Morris, P.F. Fulvio and M.Jaroniec, *J. Am. Chem. Soc.*, 2008,**130**,15210.
3 X.H.Sun, Y.F.Shi, P.Zhang, C.M.Zheng, X.Y.Zheng, F.Zhang, Y.C.Zhang, N.J.Guan, D.Y. Zhao and G.D. Stucky, *J. Am. Chem. Soc.*, 2011,**133**,14542.
4 K.An, S.Alayoglu, N.Musselwhite, S.Plamthottam, G.Melaet, A.E. Lindeman and G.A. Somorjai, *J. Am. Chem. Soc.*, 2013,**135**,16689.

5 D.H.Chen, L.Cao, T.L.Hanley and R.A.Caruso, *Adv.Funct.Mater*., 2012,**22**,1966.

6 T.Brezesinski, J.Wang, S.H.Tolbert and B.Dunn, *Nat.Mater*., 2010,**9**,146.

7 Y.Ren, Z.Ma and P.G.Bruce, *Chem. Soc. Rev*., 2012,**41**,4909.

8 Y.Wang, W.Li,X.L.Jiao and D.R.Chen, *J.Mater.Chem*. 2013,**1**,10720.

9 Q.Yuan, A.X.Yin, C.Luo, L.D.Sun, Y.W.Zhang, W.T.Duan, H.C.Liu and C.H.Yan, *J. Am. Chem. Soc*., 2008,**130**,3465.

10 Z.X.Wu, Q.Li, D.Feng, P.A.Webley and D.Y. Zhao, *J. Am. Chem. Soc*., 2010,**132**,12042.

11 A.Mitra, D.Jana and G.De, *Chem. Commun*., 2012,48,3333.

12 J.Górka, M.Jaroniec and W.L.Suchanek, *Nanoscale*., 2010,**2**,2868.

13 W.Q.Cai, J.G.Yu, C.Anand, A.Vinu and M. Jaroniec, *Chem Mater*., 2011,**23**,1147.

14 H. Li, M. Eddaoudi and M. O'Keeff, *Nature*., 1999,**402**, 276.

15 K.L. Mulfort and J.T. Hupp, *J. Am. Chem. Soc*., 2007,**129**,9604.

16 B. Sareeya, H. Satoshi and H. Masakazu, *Nat. Mater*., 2009,**8,**832.

17 B. Liu, H. Shioyama and T. Akita, *J. Am. Chem. Soc*., 2008,**130**,5390.

18 K.E.deKrafft, C.Wang and W.B. Lin, *Adv. Mater*., 2012,**24**,2014.

19 R.B.Wu, X.K.Qian, F.Yu, H.Liu, K.Zhou, J.Wei and Y.Z.Huang, *J. Mater. Chem. A*., 2013,**1**,11126.

20 T.K.Kim, K.J.Lee, J.Y.Cheon, J.H.Lee, S.H.Joo and H.R.Moon, *J. Am. Chem. Soc*., 2013,**135**,8940.

21 R.Das, P.Pachfule, R.Banerjee and P.Poddar, *Nanoscale*., 2012,**4**, 591.

22 L.Peng, J.L.Zhang, Z.M.Xue, B.X.Han, J.S.Li and G.Y.Yang, *Chem. Commun*., 2013,**49**,11695.

23 W.Xia, J.H.Zhu, W.H.Guo, L.An, D.G.Xia and R.Q.Zou, *J.Mater. Chem. A*, 2014,**2**, 11606.

24 P.Wang, H.Li, Q.Gao, P.Z.Li, X.Yao, L.Y.Bai, K.T.Nguyen, R.Q.Zou and Y.L.Zhao, *J. Mater. Chem. A*, 2014,**2**, 18731

25 W.Xia, R.Q.Zou, L.An, D.G.Xia and S.J.Guo, *Energy Environ. Sci*., 2015,**8**, 568.

26 D.D.Liu, F.N.Dai , Z.Tang , Y.Q.Liu and C.G. Liu , *Mate.Rese. Bull.*, 2015,**65**, 287.

27 D.D.Liu, F.N.Dai, X.H. Li, J.L.Liang, Y.Q.Liu and C.G.Liu, *RSC Adv.*, 2015, **5**, 15182

28 A. Comotti, S. Bracco, P. Sozzani, S. Horike, R. Matsuda and J.X. Chen, *J. Am. Chem.Soc*., 2008,**130**,13664.

29 J.Liu, F.Zhang, X.Q. Zou, G.L.Yu, N.Zhao, S.J.Fan and G.S.Zhu, *Chem. Commun*., 2013,**49**,7430.

30 I. Senkovska, F. Hoffmann, M. Fröba, J. Getzschmann,W. Böhlmann, and S. Kaskel, *Micro. Meso. Mater*., 2009,**122**, 93.